29th International Congress on Sound and Vibration
The annual congress of the International Institute of Acoustics and Vibration (IIAV)
9–13 July 2023
ICSV29

COMPARISON OF LASER DOPPLER VIBROMETRY AND DIGITAL IMAGE CORRELATION MEASUREMENT TECHNIQUES FOR APPLICATIONS IN VIBROACOUSTICS

Sebastian F. Zettel, Marco Norambuena, Ray D. Dewald and Marc Böswald
German Aerospace Center (DLR), Institute of Aeroelasticity, Göttingen, Germany
email: sebastian.zettel@dlr.de

Laser-Doppler Vibrometry (LDV) is a state-of-the-art contactless measurement technique able of capturing the velocity response at a single measurement point, up into the high-frequency range with high accuracy. With scanning LDV, even the velocity field of the surface of a test object can be observed from a sequence of repeated measurements. A 3D LDV system is able to measure all 3 spatial components of velocity, in-plane as well as out-of-plane. However, the most common 1D LDV systems are only able to measure the velocity component in the direction of the laser beam. With proper setup of the system, this corresponds to the out-of-plane component. An alternative contactless measurement technique that had arisen in the last decade is the Digital Image Correlation (DIC). This technique allows to measure the displacement fields of structures based on a full-field method using a series of images taken over time at discrete time intervals. While the measurement time of both methods highly depend on the set parameters, the DIC has the advantage that in-plane velocities are measured without additional effort. In this paper a comparison between measured data acquired using both techniques will be performed. The targeted application is conducting measurements on lightweight structures in the vibroacoustic frequency range. To this end, the upper frequency limit shall be determined, at which the DIC data quality is comparable to the LDV data, regarding out-of-plane components. Additionally, both data sets will be used to estimate structural intensity vector fields for quality and performance estimation.

Keywords: vibroacoustics, LDV, DIC, structural intensity

1. Introduction

Methods in vibroacoustics investigate the structural behaviour in the so-called mid-frequency range. This range is located between the low- and the high-frequency range. In the low-frequency range the behaviour of structures can be described using modal properties like eigenfrequencies and eigenvectors. The high-frequency range is usually described using statistical approaches, because modal analysis is not adequate anymore due to high modal density.

Depending on the size of the structure, measurements in the low frequency range require only a few measurement points to capture the first distinctive global mode shapes. In the mid-frequency range the number of points increases drastically in order to capture the smaller wavelengths resulting from local mode shapes. Commonly, measurements in the mid-frequency range are performed using Laser-Doppler-Vibrometer (LDV). LDV systems allow for the acquisition of high-density velocity fields without effects of mass loading and accompanying frequency shifts of eigenfrequencies. Another effective technique uses a rowing grid of accelerometers [1]. However, this technique is only applicable for larger structures on which the additional sensor mass has no relevant effect regarding its response.

While LDVs have high accuracy at a single measurement point, the measurement time increases linearly with the number of measurement points. For larger objects like aircraft fuselages, this may lead to

a very time-consuming process. A measurement technique which allows to perform measurements of larger scale in shorter time is Digital Image Correlation (DIC). The DIC utilizes the evaluation of consecutive captured images with fixed time-intervals of the time-variant deformation of a structure. A speckle pattern applied on the surface of the structure allows to track the deformation of individual points over time [2]. Currently, DIC in structural mechanics is mostly only used for static deformation measurements or modal analysis applications [3,4]. Advantages of DIC are, e.g. lower costs compared to LDVs (approximately a factor of two for single-point LDV) and simultaneous measurement of out-of-plane and in-plane components [5].

In this paper a comparison of these two measurement techniques is performed in order to determine the frequency range in which the DIC can be used for vibroacoustic measurements. For this purpose, measurements on a laboratory structure developed at the German Aerospace Center (DLR) are performed. The DIC data is correlated with LDV measurements, which will act as a ground truth due to the superior accuracy, using the Energy Correlation Criterion (ECC). Additionally, evaluations using the estimation if structural intensity (STI) are performed to check the applicability of DIC measurements for this analysis method. The goal of these investigations is to enable the DIC system for vibroacoustic measurement campaigns on large structures, quick measurements and to simply extend the portfolio of available measurement techniques in the department.

Chapter 2 covers the experimental setups for LDV and DIC measurement as well as the laboratory structure. Chapter 3 will describe the ECC and present the results of the correlation. Chapter 4 shows an evaluation of the measurement data utilizing structural intensity (STI).

2. Experimental setup

The experimental setup uses a laboratory structure called vibro-plate. The vibro-plate was excited by an electro-dynamic shaker. The response of the plate was measured using LDV and DIC. The LDV measurement has been performed in another project and the data has been re-used for correlation in this publication. Therefore, the upper and lower limit of the measured frequency range of LDV and DIC differ from each other.

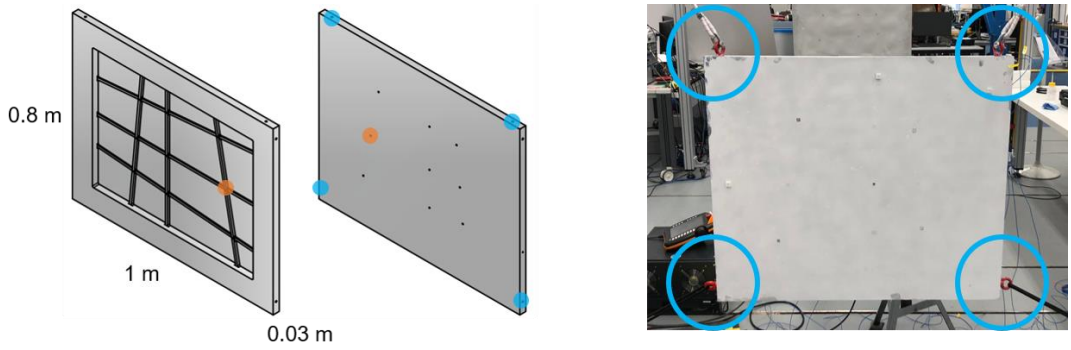

Figure 2-1: Laboratory structure, a) with dimensions and indicators for suspension and excitation, orange: excitation point, blue: suspension attachments, b) bungee suspension [6]

The vibro-plate has been milled from a solid 30mm thick aluminium plate. The central part of the plate consists of 9 individual skin fields of 1mm thickness. The aluminium plate is stiffened with bars (i.e. ribs) encircled in a thick frame which acts as a fixed boundary condition. The frame of the plate has a thickness of 30 mm while the vertical stiffeners have a thickness of 11 mm and the horizontal stiffeners 6 mm. Figure 2-1 a) shows the plate from both sides. Since the plate was manufactured from a monolithic block of aluminium, it has no joints which could potentially add damping due to friction. Additionally,

the arrangement of the stiffening bars is chosen in a way that no symmetries exist which allows unique transfer paths to emerge. The idea was to create a structure with vibro-acoustic features close to those of a real-world aircraft fuselage while eliminating as many uncertainties as possible. In order to attach shakers to the vibro-plate, drilling holes are present in every stiffener crossing. The drill holes in the corners of the frame of the plate allow to attach suspensions. During the LDV measurement, the vibro-plate was suspended by bungee ropes on all four corners, see Figure 2-1 b). For the DIC measurement the plate was suspended only on the two upper corners.

As already mentioned the LDV measurement was taken during another project which made it necessary to attach suspensions on all four corners. Currently, the vibro-plate is used in a project which uses a suspension only on the two upper corners. This is the reason the DIC measurement was taken with the plate being only suspended on two corners in order to not alter the current system setup.

The measurement with the LDV was performed by using a specific scanning unit developed at DLR [7]. This system allows to perform automated measurements. A total of 19486 equally spaced points were measured on the flat backside of the vibro-plate covering only the skin-field area of the plate. During the LDV measurement, an electro-dynamic shaker was used to excite the plate with a random crest optimized (crest factor = 1.6) signal limited to the frequency range of 50 – 5000 Hz at the location indicated in Figure 2-1 a). An acquisition time of 5 seconds per point was used which resulted in a total measurement time of roughly 27 hours. A sample rate of 10240 Hz was used. The acquired time-domain data of the velocity field was transformed to the frequency domain using the Welch's method (i.e. periodogram approach) [7]. A frequency resolution of 5 Hz was chosen.

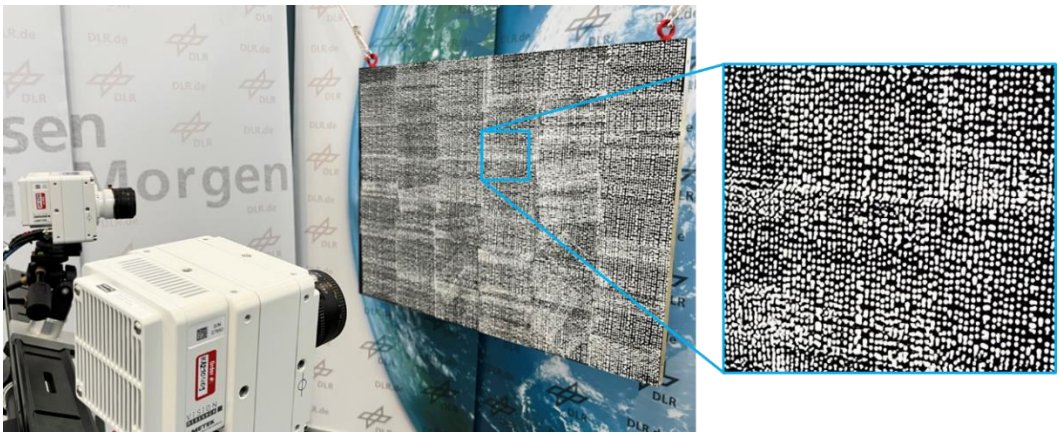

Figure 2-2 : DIC measurement setup with speckle pattern close-up

For the DIC measurement a LaVision system has been used with two high-speed cameras (Phantom Veo 440) with 4 MP each and a frame-rate of 1100 frames per second were used. The cameras were located at 2.6 m distance from the structure and had a horizontal separation of 0.56 m. An overview of the setup can be seen in Figure 2-2.

The field of view of the cameras was trimmed to the plates skin-field area leaving out the thick surrounding frame which resulted in 1664 x 1244 pixels. This increased the sample rate from 1100 frames per second to 2000 frames per second. This allowed to measure up to a frequency of 1000 Hz. The internal memory of the cameras allowed to capture a maximum of 5866 images at this resolution. This resulted in a total measurement time of 2.93 seconds. In total five measurements with a duration of 2.93 seconds were performed to create a longer response signal. This allowed to perform more averaging within the Welch's method and therefore increase the signal-to-noise ration. The processing of the acquired images took roughly 5 hours. The frequency resolution was set to 5 Hz as is was for the LDV data. The excitation was performed at the same location with the same kind of signal but limited to a frequency range of 10 – 1000 Hz. The resulting displacement FRFs were transformed to velocity in the

frequency-domain by multiplying with the imaginary frequency vector $\omega_{imag} = i \cdot 2\pi \cdot f$ with the unit [rad/s].

The vibro-plate was painted with a random speckle pattern with a distribution of black and white with approximately 50% as shown in Figure 2-2. Additionally, light sources were directed on to the plate to increase contrast. Based on the speckle pattern and the chosen DIC system parameters for the measurement, a total of 11224 equally spaced measurement points resulted.

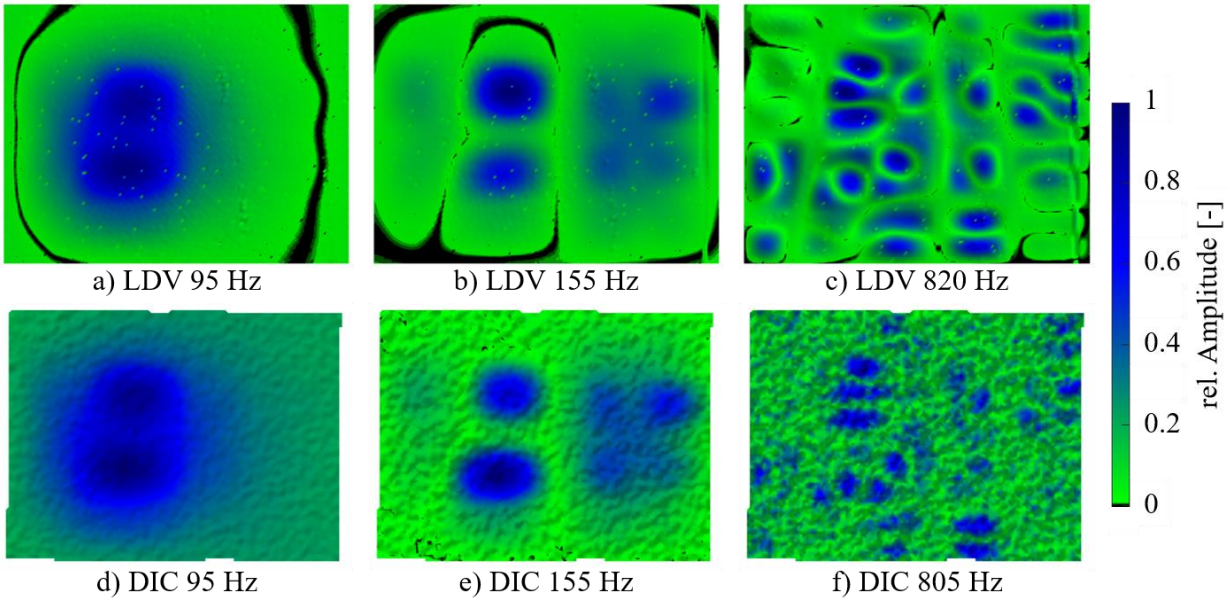

Figure 2-3: Examples of operational deflection shapes measured with LDV and DIC

Figure 2-3 shows exemplary operational deflection shapes (ODS) at discrete frequencies for the LDV and DIC datasets. In case of the DIC dataset only out-of-plane components are used to present comparable ODS. In a visual comparison it becomes clear that both measurement techniques show similar ODS at the same frequencies. In the upper frequency range a slight frequency shift starts to emerge. The reason might be the difference in suspension points of the plate. However, the frequency shift is below 2% and thus neglectable. The ODS from the LDV dataset show a very high signal-to-noise ratio over all frequencies. While the ODS of the DIC dataset are similar to the ones of the LDV, the signal-to-noise ratio is lower. The principal deflections of the ODS are superimposed by artificial deflections of much shorter wavelength.

3. Correlation of operational deflection shapes with ECC

The ECC is a correlation method developed at the DLR and is a combination of the vector correlation described in Equation 1 and the basic idea of the Statistical Energy Analysis (SEA). It follows a short summary based on Biedermann et al. [8].

The investigated structure is split up into a discrete number of subcomponents, e.g. an equally spaced grid of squares. For every measurement point i in the respective subcomponents the kinetic energy is calculated based on the amplitude of velocity $\hat{v}_i$ and the partial mass m_i for a discrete frequency ω.

$$E_{kin}(\mathrm{i}, \omega) = \frac{1}{2}\, m_i\, \hat{v}_i{}^2(\omega) \tag{1}$$

For every subcomponent k the total kinetic energy is then calculated by a summation of the corresponding points and over all spectral lines e.g. in the respective 1/3-octave frequency bands n

$$E_{kin}(k,n) = \sum_{\omega=1}^{\Omega} \sum_{i=1}^{I} E_{kin}(i,\omega)\ \Delta\omega \tag{2}$$

where $\Delta\omega$ describes the frequency resolution.

The vector $\{E_{kin}(\mathrm{n})\}$ containing the values of total kinetic energies for all subcomponents k = 1, 2, …, K at the discrete frequency band *n* is then used in a vector correlation for a set of available spectral lines

$$ECC(n) = \frac{\left(\{E^a_{kin}(n)\}^T \{E^b_{kin}(n)\}\right)^2}{\{E^a_{kin}(n)\}^T \{E^b_{kin}(n)\} \{E^a_{kin}(n)\}^T \{E^b_{kin}(n)\}} \quad \text{with} \quad n = 1, 2, \dots, N. \tag{3}$$

As the ECC is based on the vector correlation the resulting correlation values also range from 0, showing no linear dependencies, and 1, for a collinearity, between the energy vectors. A value above 0.8 is indicated as a high level of linear dependency between compared datasets [8]. For the following evaluations this limit will be adopted.

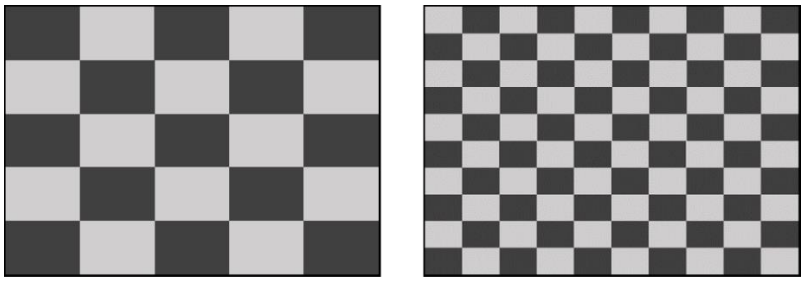

a) b)

Figure 3-1: ECC subcomponents size examples, a) 5 x 5, b) 10 x 10

The inclusion of spatial and spectral integration makes the ECC more robust against uncertainties, i.e. inconsistent measurement points, geometric deviations and slightly varying material properties. However, there is no clear guidance on how the size of the subcomponents shall be chosen. The limiting cases are first, a size of subcomponents which are so small that they coincide with the actual measurement point density. In this case the ECC results would converge towards the more commonly known Frequency Domain Assurance Criterion (FDAC) which performs a point-by-point correlation of ODS. Second, a subcomponent which has the dimension of the structure itself. This would result in a correlation value of 1 and would thus be inconclusive.

Therefore, a statistical evaluation of a set of subcomponent sizes is recommended. This approach indicates if the datasets have a high dependency on the subcomponent size in certain frequency bands. If the standard deviation is small it shows a strong confidence that the ECC correlation is valid while the confidence in the results decrease with increasing standard deviations. In this paper six different subcomponents sizes were considered. The subcomponents ranged from 5 x 5 to 10 x 10 (with an increment of 1) equally spaced rectangles covering the plate geometry, see Figure 3-1.

In The ECC evaluation of the two datasets from chapter 2 are presented. The correlation results stay above 0.8 up to 630 Hz. Only from here the correlation values start to decrease strongly with additionally increasing standard deviations.

Based on the ECC values it can be said that the datasets show a strong correlation up to frequencies including the 630 Hz band. The reasons are mean correlation values above 0.8 and standard deviations which are small. Additionally, the lower limits of the standard deviations are also above 0.8. The 800 Hz and 1000 Hz frequency bands however show mean correlation values below 0.8 and standard deviation with a wide range and thus even lower limits. The reason for this is probably the decreasing signal-to-

noise ratio due to wavelength of the structural response which coincide with the wavelength of the noise. These results show that the DIC system currently reaches its performance limit, in case of the vibro-plate, in the 630 Hz band. However, this is only the case for the currently chosen parameters of the DIC measurement.

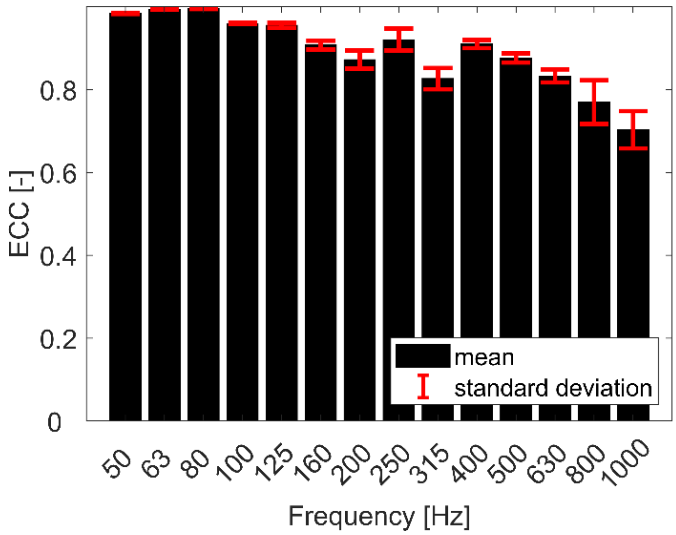

Figure 3-2: Energy correlation criterion evaluation with standard deviation

In order to allow the transfer of these results to similar structures of other dimension, a reference is made to chapter 4 of Zettel et al. [9] which contains a frequency scaling diagram based on geometric and material parameters.

4. Estimation and comparison of structural intensity vector fields

The STI is a vector quantity which represents the amount of vibrational power transmitted through a structure of solid material per cross-sectional area in the direction of the flow. In order to calculate the STI for an arbitrary point of a structure the complex-conjugate velocity vector and its stress tensor need to be known [10].

It is straightforward to calculate the STI vectors based on numerical data, e.g. from FEM results, because all the required data is available. This is not the case for experimental data. A great effort is necessary to estimate missing response values such as rotations about in-plane axis and tensions. An approach that emerged in the last years utilizes the mapping of experimental data to a FEM mesh. This approach allows to calculate element stresses and additionally to estimate missing rotational DOF of the in-plane axes which are important to calculate shear stresses. The approach uses the FEM process to calculate element stresses based on nodal displacements. However, there is no need for a solver as the displacement data is already existing in form of the mapped experimental data. It is necessary to setup a mesh of experimental response points and to establish shape functions as the FEM does. This provides a theory to calculate the strains for the respective elements used, e.g. Mindlin-Reissner theory for thin plates [11]. When the material law is known, like it is for the vibro-plate made from aluminium, the required stresses can be determined from the strains.

The STI vector fields were calculated using a triangular mesh. The mesh nodes are the respective points of the LDV and DIC measurement grid. Only out-of-plane components were used to present comparable vector fields.

In general, the STI vector fields for LDV and DIC did not show big similarities over the investigated frequency range. This is related to the lower signal-to-noise ratio of the DIC data already mentioned in chapter 3. Because of the higher noise levels of the DIC data, a kind of background power flow emerges

in the STI vector fields which is not apparent in the vector fields of the LDV data. In Figure 4-1 a comparison of STI vector fields at a discrete frequency of 155 Hz is presented. Comparing Figure 4-1 a) and b) shows that the main power flow is located at the same place of the plate. However, while the rest of the plate shows a power flow close to zero in the LDV data, this is not the case for the DIC data. The noise of the DIC data results in STI values with a higher relative amplitude than they should have. Also, in the zooms (Figure 4-1 c) and d)) it becomes apparent that the vector fields show strong dissimilarities.

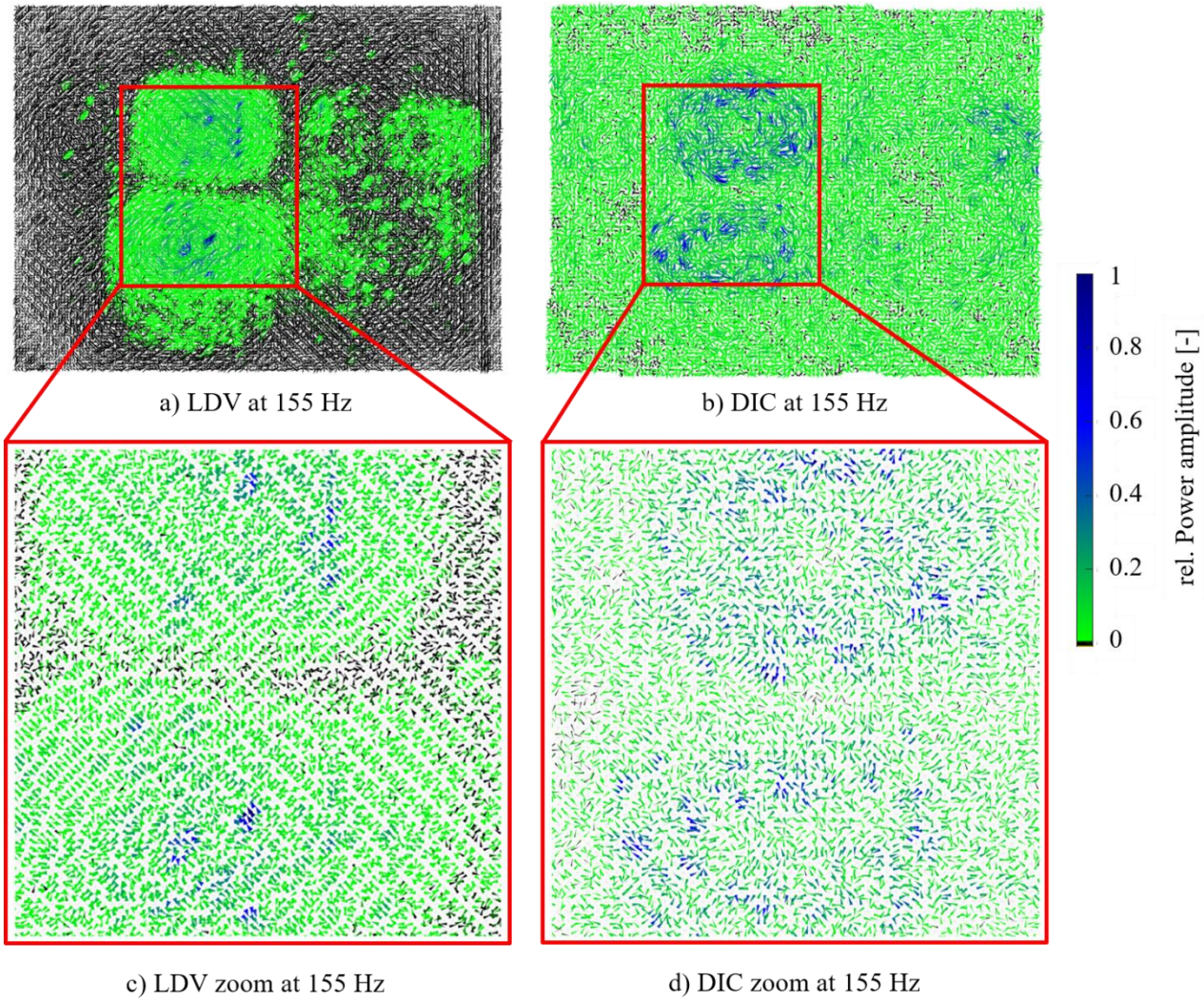

Figure 4-1: Structural intensity vector fields estimated from LDV and DIC data with zoom

The Discrete Hodge Helmholtz Decomposition (DHHD) is a commonly used approach to analyse STI vector fields. It allows to decompose the vector fields into divergence and rotational parts. The divergence part indicates sources and sinks of STI vector fields while the rotational part indicates parts of the vector field which do not have a distinct source or sink [12]. The calculation of the DHHD for the LDV data worked properly. In case of the DIC data however, the calculation resulted in meaningless results probably due to the noise. Therefore, a comparison of decomposed vector fields between LDV and DIC was not possible. With the currently chosen parameters the measurement data of the DIC system is not capable to be used for STI evaluations.

5. Conclusion & Outlook

The structural response of a laboratory structure was measured with a LDV and a DIC measurement system. A visual comparison of the ODS of both datasets showed similar global deformations. However,

the DIC data showed a significant lower signal-to-noise ration. The comparison of the two datasets using the ECC, which is a correlation method robust against noise, showed acceptable correlation results up to the 630 Hz 1/3-octave frequency band. Above the 630 Hz band the correlation started to decrease rapidly.

Furthermore, an evaluation utilizing the estimation of STI from the two respective datasets was performed. The visual comparison of the vector fields indicated that the noise level of the DIC datasets was too high for a clear comparison of the STI vector fields. In comparison to the STI vector field of the LDV dataset the DIC dataset showed a background power flow of relative power amplitudes because of the lower signal-to-noise ratio. Additionally, the calculation of a DHHD was not possible also due to the noise level of the DIC dataset. Therefore, it is not possible to perform valid STI evaluations with the currently chosen DIC measurement parameters.

For future measurements with the DIC it is important to increase the signal-to-noise ratio. In order to do so, the number of consecutive DIC measurements could be increased to create a longer response signal which allows more averages during FRF processing. However, the question remains what the least amount of measurements is to increase the signal-to-noise ratio to a sufficient level. The reason is the extensive amount of memory the DIC requires due to the utilized high-resolution images.

REFERENCES

1 Winter, R., Sinske, J., Norambuena, M., Zettel, S.F. *High-resolution vibroacoustic measurement and analysis of the DLR ISTAR aircraft to assess engine-induced cabin noise*. 51st INTER-NOISE 2022, 21.-24. Aug. 2022, Glasgow, UK (2022).

2 Sutton, M. A., Orteu, J.J., Scheier, H.W. *Image Correlation for Shape, Motion and Deformation Measurements*. Springer Science, 978-0-387-78746-6, (2009).

3 Wang, W., Mottershead, J.E., Ihle, A., Siebert, T., Schubach, H.R. *Finite element model updating from full-field vibration measurement using digital image correlation*. Journal of Sound and Vibration 330(8): 1599-1620, (2011).

4 Hild, S., Roux, S. *Digital Image Correlation: from Displacement Measurement to Identification of Elastic Properties – a Review.* Strain 42: 69-80, (2006).

5 Reu, P. L., Rohe, D.P., Jacobs, L.D. *Comparison of DIC and LDV for practical vibration and modal measurements*. Mechanical Systems and Signal Processing 86: 2-16, (2017).

6 Dewald, R.D. *Modellierung und Modellvalidierung einer rippenversteiften Platte für vibroakustische Fragestellungen*. Masterarbeit, Institut für Dynamik und Schwingungen, Leibniz Universität Hannover, (2020).

7 Brandt, A., Manzoni, S. *Introduction to spectral and correlation analysis: Basic measurements and methods*. In R. Allemang and Peter Avitabile, editors, Handbook of Experimental Structural Dynamics, pages 1–30. Springer New York, New York, NY, 2020.

8 Biedermann, J., Winter, R., Wandel, M. and Böswald, M. *Energy based correlation criteria in the mid-frequency range*. Journal of Sound and Vibration. 400: 457-480, (2017).

9 Zettel, S.F. et al. *Finite Element Method and Dynamical Energy Analysis in Vibro-acoustics – A comparative study*. 50th INTER-NOISE 2021, 1st – 5th Aug. 2021, Washington D.C., USA (2021).

10 Hambric, S. A. *Power flow and mechanical intensity calculations in structural finite element analysis.* Journal of Vibration and Acoustics 112(4): 542-549, (1990).

11 Biedermann, J., et al. *A hybrid numerical and experimental approach for structural intensity analysis of stiffened lightweight structures*. ISMA. Leuven: 4101-4115, (2018).

12 Guo, Q., et al. *Efficient Hodge–Helmholtz decomposition of motion fields.* Journal of Pattern Recognition Letters 26(4): 493-501, (2005).